Saudi Journal of Engineering and Technology **ISSN 2415-6272 (Print)**
Scholars Middle East Publishers **ISSN 2415-6264 (Online)**
Dubai, United Arab Emirates
Website: http://scholarsmepub.com/

Design and Evaluation of Compressive Strength of Wood Ash Particles (Hardwood) Reinforced Polypropylene (WARPP) Composite Material for Improved Energy Absorption in Crash Energy Management

Aguh Patrick Sunday[1], Ejikeme Ifeanyi Romanus[2]
[1]Department of Industrial Production Engineering, Nnamdi Azikiwe University, Awka, Anambra State, Nigeria
[2]Office of the Commissioner, Ministry of Environment, Beautification and Ecology, Awka, Anambra State, Nigeria

***Corresponding author**
Aguh Patrick Sunday

Article History
Received: 25.08.2017
Accepted: 05.10.2017
Published: 30.11.2017

DOI:
10.21276/sjeat.2017.2.11.6

Abstract: This paper utilized the compressive tests results to examine the crushing behaviour of wood ash particles (hardwood) reinforced polypropylene (WARPP) for crash energy management. The study employed Taguchi method of experimental design to generate data for the work. Gauss – Legendre two point rules was used to evaluate the area under the stress – strain curves which measured the amount of energy absorbed per unit volume of sample. With this evaluation method the highest ultimate strength of 10.5384J/m^3 with corresponding work absorption of 1.1 x 10^{-5}J was obtained. Also established with the compression data was the specific energy absorption of 0.01038J/Kg and compressive modulus of 4.9885N/mm2.
Keywords: Design of experiment, Gauss – Legendre two point rule, Energy absorption, Crush force efficiency

INTRODUCTION

The energy absorption capability of a composite material is important in structural damage caused by accidental collision. Accidental collision can be observed or experienced in moving objects such as vehicles. Composite structures are capable of increased energy absorption over metallic structures and therefore are exploited within automotive structure [1]. Energy absorption for a well-designed composite structures occur through a series of processes involving splitting and brittle fracturing while metals fail by folding and buckling mechanisms [2,3].

The energy absorption processes that involve splitting and brittle fracturing is an important new study that focuses on the way in which structures and materials can be designed to absorb kinetic energy in a controlled and predictable manner. An investigation into energy absorption systems require the understanding of engineering materials, structural mechanics, and theory of plasticity and impact dynamics [4].

The energy absorption capability of a composite material is critical to the development of improved energy dissipating devices. Energy absorption generally is dependent on many parameters such as fibre type, matrix type, fibre architecture, specimen geometry, processing conditions, fibre volume fraction and testing speed. Changes in these parameters can cause subsequent changes in the specific energy absorption (SEA) of the composite materials up to a factor of 2 [5].

The characteristics of composites, such as high stiffness – to – weight and strength – to – weight ratios, fatigue resistance and corrosion resistance make them attractive in many technological applications like in aerospace, automobile and medical industries. Polymer composites are subjected to varying mechanical forces during manufacture and in service.

Energy absorption of composite material can be studied by evaluating the compressive strength of the composite material subjected to compression loading. Stressing in compression produces a slow and indefinite yielding that seldom leads to failure unlike in tensile loading that usually results in a clear – cut failure [6]. Because of this phenomenon, compressive strength is customarily expressed as the amount of stress required to deform a standard plastic test specimen to a certain strain. Compressive modulus is not always reported because defining stress at a given strain is equivalent to reporting a secant modulus. A secant modulus is the ratio of stress to corresponding strain at any point on the stress – strain curve.

In this work, crushing is considered the failure mode that governs the mechanical behaviour of WARPP composite material in service. Crush test of energy absorbing materials can be performed under two conditions:

- Quasi – static condition and
- Impact condition [5].

Crush test of WARPP samples was performed under quasi – static condition. In quasi – static testing, the specimen is crushed at a constant speed. The major advantage of quasi – static test is that it is used to study failure mechanisms in composites by selection of appropriate crush speed.

Design of Experiments

While the technique of trial – and – error can be used to identify the influences of particle size and volume fraction on the crushing properties of WARPP, such method requires a huge number of experimental runs to minimize the effect of output variability in the presence of noise (output variability mean variations due to component size variations, different environmental conditions, etc.). One way of overcoming this problem is to employ design of experiments (DOE) approach.

Design of experiment is a structured method for determining the relationship between process inputs and process outputs. It is important to note that the number of experimental trials required for a certain experiment must be greater than or equal to (≥) the system degree of freedom (Anthony and Capon, 1998). System degree of freedom is derived from the formula:

DOF = 1 + (number of variables) x (number of levels – 1).

Design of experiments (DOEs) is based on a matrix of experiments called orthogonal arrays (OA). These are a set of experiments where the factors and levels used as the settings of various parameters are changed according to the matrix [7]. They are called orthogonal because the set of experiments are balanced (that is each pair – wise combination of values of factors occur in the same number of trials. A typical orthogonal array used in this work is presented in Table I.

Table-1: L_9 $(3)^4$ Orthogonal Array

Expt ..NO .	*Particle size (A)*	*Volume fraction (B)*	*Injection force (C)*	*Operating temp .(D)*
1	1	1	1	1
2	1	2	2	2
3	1	3	3	3
4	2	1	2	3
5	2	2	3	1
6	2	3	1	2
7	3	1	3	2
8	3	2	1	3
9	3	3	2	1

There are four (4) factors at three (3) levels. The configuration in the table is called an "L_9" design, with the 9 indicating that nine experiments are to be carried out to study four variables (factors) at three levels. For convenience, we denote the values of the variables as levels 1, 2 and 3.

A complete investigation requires (3)4 = 81 experiments. With the application of DOF according to Anthony and Capon [8], the number of experimental evaluation reduces to 9.

MATERIALS AND METHOD

The crush test samples used in this research are manufactured from thermoplastic polymer, polypropylene (PP) resin as matrix material and wood ash particles as filler material. Polypropylene, a linear hydrocarbon polymer was sourced from a resin chemical commercial outfit named POKEZ chemicals at Onitsha, while the wood ash particles were obtained from 10Kg mass of sawdust. The sawdust was burnt and allowed to smouldered in an open space at ambient temp. for 12 hrs.

The method applied involve the use of Aguh [9] data of replicated samples of WARPP composites tested for compressive failure and the application of Gauss – Legendre two – point rule in the evaluation of absorbed energy. The sample test replication apparatus is presented in Figure 1a & b.

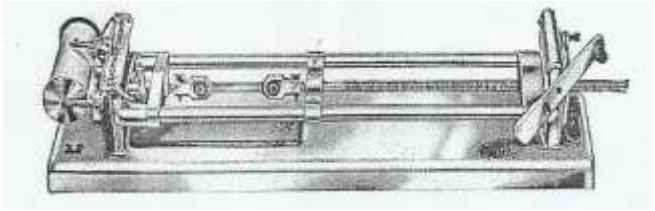

Fig-1a: Pictorial diagram of Hounsfield extensometer experimental rig
(Source: Zhang Sam, 2008).

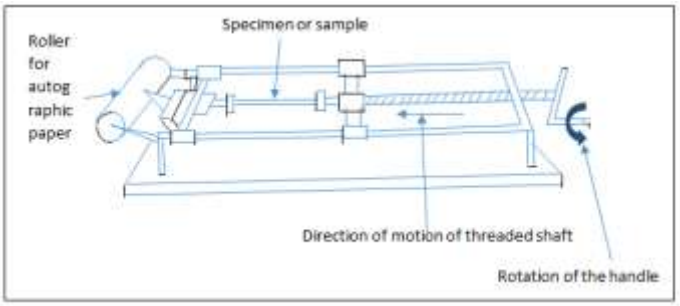

Fig-1b: Sketch of the compression test set up of Monsanto extensometer.

In the Aguh [9] work, all the replications of the primary data, Table 3a were combined in evaluation to obtain the mean values presented in Table 3b.

Table-2: A dimensional property of the sample replicates (compression)

Sample particle size (*mm*)	*Volume fraction* (%)	*Mass* (*g*)	*Length* (*cm*)	*Width* (*cm*)	*Thickness* (*cm*)	*Cross sectional area* (cm^2)	*Density* (g/cm^3)
0.25	5	3.745	2	0.6	0.3	0.18	10.403
	35	3.969	2	0.6	0.3	0.18	11.025
	60	4.156	2	0.6	0.3	0.18	11.544
0.80	5	3.745	2	0.6	0.3	0.18	10.403
	35	3.969	2	0.6	0.3	0.18	11.025
	60	4.156	2	0.6	0.3	0.18	11.544
1.40	5	3.745	2	0.6	0.3	0.18	10.403
	35	3.969	2	0.6	0.3	0.18	11.025
	60	4.156	2	0.6	0.3	0.18	11.544

Table-3a: Primary data of compressive test of WARPP materials

Sample particle size (mm)	*Vol. fract. (%)*	*Comp. force (N) Trial 1*	*Comp. deform. (mm) Trial 1*	*Comp. force (N) Trial 2*	*Comp. deform. (mm) Trial 2*	*Comp. force (N) Trial 3*	*Comp. deform. (mm) Trial 3*	*Comp. force (N) Trial 4*	*Comp. deform. (mm) Trial 4*	*Comp. force (N) Trial 5*	*Comp. deform. (mm) Trial 5*	*Mean comp. force (N)*	*Mean comp. deform. (mm)*
0.25	5	0.00	0.00	0.00	0.00	0.00	0.00	0.00	0.00	0.00	0.00	0.00	0.00
		300	0.125	200	0.125	250	0.125	225	0.125	275	0.125	250	0.125
		500	0.250	500	0.500	535	0.313	600	0.438	365	0.375	500	0.375
		850	1.250	900	1.375	875	1.313	862.5	1.281	887.5	1.344	875	1.313
		1200	2.500	1100	2.625	1175	2.561	1125	2.531	1150	2.593	1150	2.562
		1800	4.375	1700	4.250	1775	4.311	1750	4.281	1725	4.343	1750	4.312
		1800	5.625	1700	5.250	1775	5.594	1750	5.422	1725	5.610	1750	5.500
0.25	35	0.00	0.00	0.00	0.00	0.00	0.00	0.00	0.00	0.00	0.00	0.00	0.00
		500	0.125	400	0.125	450	0.125	425	0.125	475	0.125	450	0.125
		800	0.375	500	0.375	650	0.375	575	0.375	725	0.375	650	0.375
		1180	1.125	1080	0.875	1130	1.000	1105	0.938	1155	1.063	1130	1.000
		1420	2.125	1540	1.875	1480	2.000	1450	1.938	1510	2.063	1480	2.000
		1900	3.250	1800	3.750	1850	3.500	1825	3.375	1875	3.625	1850	3.500
		1900	4.750	2000	5.375	1966.8	5.061	1933.4	4.906	1950	5.218	1950	5.062
0.25	60	0.00	0.00	0.00	0.00	0.00	0.00	0.00	0.00	0.00	0.00	0.00	0.00
		280	0.125	300	0.125	290	0.125	285	0.125	295	0.125	290	0.125
		550	0.250	600	0.375	575	0.311	562.5	0.281	587.5	0.343	575	0.312
		1800	0.750	1750	0.750	1775	0.750	1762.5	0.750	1787.5	0.750	1775	0.750
		3550	1.250	2900	1.750	3062.5	1.500	3225	1.375	3387.5	1.625	3225	1.500
		5350	2.000	4250	2.500	4800	2.250	4525	2.125	5075	2.375	4800	2.250

Sample particle size (mm)	*Vol. fract. (%)*	*Comp. force (N) Trial 1*	*Comp. deform. (mm) Trial 1*	*Comp. force (N) Trial 2*	*Comp. deform. (mm) Trial 2*	*Comp. force (N) Trial 3*	*Comp. deform. (mm) Trial 3*	*Comp. force (N) Trial 4*	*Comp. deform. (mm) Trial 4*	*Comp. force (N) Trial 5*	*Comp. deform. (mm) Trial 5*	*Mean comp. force (N)*	*Mean comp. deform. (mm)*
0.80	5	0.00	0.00	0.00	0.00	0.00	0.00	0.00	0.00	0.00	0.00	0.00	0.00
		400	0.125	350	0.125	375	0.125	362.5	0.125	387.5	0.125	375	0.125
		650	0.250	550	0.250	600	0.250	575	0.250	625	0.250	600	0.250
		1210	1.000	1100	0.875	1155	0.939	1127.5	0.907	1182.5	0.970	1155	0.938
		1550	2.125	1460	1.500	1505	1.814	1482.5	1.657	1527.5	1.970	1505	1.813
		1820	3.500	1750	2.750	1785	3.125	1767.5	2.938	1802.5	3.313	1785	3.125
		1880	4.750	2050	4.125	1993	4.439	1936.5	4.282	1965	4.595	1965	4.438
0.80	35	0.00	0.00	0.00	0.00	0.00	0.00	0.00	0.00	0.00	0.00	0.00	0.00
		150	0.125	200	0.125	174.99	0.125	162.5	0.125	187.5	0.125	175	0.125
		280	1.000	350	0.250	315	0.625	297.5	0.438	332.5	0.813	315	0.625
		450	1.875	491.16	0.375	351.00	1.125	400.5	0.750	532.32	1.500	445	1.125
		450	4.000	491.16	0.525	351.00	2.264	400.5	1.395	532.32	3.132	445	2.263
0.80	60	0.00	0.00	0.00	0.00	0.00	0.00	0.00	0.00	0.00	0.00	0.00	0.00
		200	0.250	200	0.125	199.99	0.189	200	0.157	200	0.220	200	0.188
		300	0.625	550	0.375	425	0.500	362.5	0.438	487.5	0.563	425	0.500
		500	1.375	1060	0.875	780	1.125	640	1.000	920	1.250	780	1.125
		950	2.625	1380	1.625	1165	2.125	1057.5	1.875	1273.5	2.375	1165	2.125
		1200	4.500	1380	3.375	1290	3.939	1245	3.657	1335	4.220	1290	3.938

Sample particle size (mm)	*Vol. fract. (%)*	*Comp. force (N) Trial 1*	*Comp. deform. (mm) Trial 1*	*Comp. force (N) Trial 2*	*Comp. deform. (mm) Trial 2*	*Comp. force (N) Trial 3*	*Comp. deform. (mm) Trial 3*	*Comp. force (N) Trial 4*	*Comp. deform. (mm) Trial 4*	*Comp. force (N) Trial 5*	*Comp. deform. (mm) Trial 5*	*Mean comp. force (N)*	*Mean comp. deform. (mm)*
1.40	5	0.00 400 600 1100 1350 1500	0.00 0.125 0.250 0.625 2.000 3.250	0.00 500 800 1300 1600 1600	0.00 0.125 0.250 1.000 2.500 4.250	0.00 449 .98 700 1200 1474 .98 1550	0.00 0.125 0.250 0.814 2.250 3.748	0.00 425 650 1150 1412 .5 1525	0.00 0.125 0.250 0.720 2.125 3.499	0.00 474 .99 750 1250 .01 1537 .5 1575	0.00 0.125 0.250 0.907 2.375 3.999	0.00 449 .98 700 1200 .01 1474 .99 1550	0.00 0.125 0.250 0.813 2.250 3.749
1.40	35	0.00 400 850 1100 1100	0.00 0.125 0.500 0.625 1.375	0.00 450 800 1000 1000	0.00 0.125 0.875 1.625 3.125	0.00 425 824 .91 1049 .99 1049 .99	0.00 0.125 0.686 1.125 2.250	0.00 412 .5 812 .46 1024 .99 1024 .99	0.00 0.125 0.593 0.875 1.813	0.00 437 .5 837 .46 1074 .99 1074 .99	0.00 0.125 0.781 1.375 2.688	0.00 425 824 .99 1049 .99 1049 .99	0.00 0.125 0.687 1.125 2.250
1.40	60	0.00 520 950 1200 1649 .99 1740 1800	0.00 0.125 0.625 1.500 3.250 4.375 6.000	0.00 300 820 950 1200 1800 1800	0.00 0.125 0.250 1.250 2.500 4.375 5.625	0.00 410 885 1075 1499 .99 1719 .99 1800	0.00 0.125 0.438 1.375 2.875 4.375 5.813	0.00 740 .1 1080 .03 1450 .02 1349 .99 1760 1800	0.00 0.125 1.000 1.750 4.000 4.375 6.375	0.00 630 .05 1015 1325 .01 1800 1730 1800	0.00 0.125 0.813 1.625 3.625 4.375 6.188	0.00 520 950 .02 1200 .01 1499 .99 1750 1800	0.00 0.125 0.625 1.500 3.250 4.375 6.000

Table-3b: Mean stress & mean strain of experimental result of compression test of WARPP

Sample Particle Size (mm)	Volume Fraction (%)	Mean Compressive Stress (N/mm^2)	Mean Compressive Strain
0.25	5	0.00 23.8889 27.7778 48.6110 66.1109 97.2220 97.2220	0.00 0.00216 0.00647 0.02263 0.04418 0.07435 0.09475
0.25	35	0.00 25.0000 36.1105 62.7775 82.2215 102.7775 108.3330	0.00 0.00216 0.00647 0.01724 0.03448 0.06035 0.08728
0.25	60	0.00 16.1110 31.9443 98.6110 179.1670 266.6667 290.2780	0.00 0.00216 0.00538 0.01293 0.02586 0.03879 0.05819
0.80	5	0.00 20.8300 33.3340 64.1670 83.6110 99.1670 109.1670	0.00 0.00216 0.00431 0.01617 0.03125 0.05388 0.07651
0.80	35	0.00 9.7220	0.00 0.00216

		17.5000 24.7220 24.7220	0.01078 0.01940 0.03901
0.80	60	0.00 11.1110 23.6110 43.3340 64.7220 71.6670	0.00 0.00324 0.00862 0.01940 0.03664 0.06789
1.40	5	0.00 24.9990 38.8889 66.6670 81.9440 86.1110	0.00 0.00216 0.00431 0.01401 0.03879 0.06463
1.40	35	0.00 23.6110 45.8330 58.3330 58.3330	0.00 0.00216 0.01185 0.01940 0.03879
1.40	60	0.00 28.8889 52.7790 66.6670 83.3330 97.2220 100.0000	0.00 0.00216 0.01078 0.02586 0.05603 0.07543 0.10345

Each of the samples replications having the dimensional properties described in Table 2 were subjected to compression loading individually in the testing kit of Monsanto extensometer (Figure 1a & b). A constant beam load of 1000Kgf (10KN) was applied each time by the operation of operating handle. Readings of displacements vs. loads were obtained from the autographic recorder and tabulated as presented in Table 3a. The evaluated values of the samples presented in Table 3b was used in this study for analysis.

Evaluation of absorbed energy of WARPP samples in compression using Gauss – Legendre two point rules

Figures 2 – 10 depict the stress – strain curves of compression test data of Table 3b. The third order polynomial equations shown in the curves define the equations of the curves obtained by the plot of stress vs. strain. The area under the curves was estimated by the application of Gauss – Legendre two point rule that is exact for third order function [10]. The polynomial equations of the figures were evaluated in line with the method of Ihueze and Enetanya [4]. The method estimated the work or energy absorption of WARPP samples at ultimate strength and or at fracture. The solid lines in the plotted curves show the actual data curve while the broken line curves are the fitted curves.

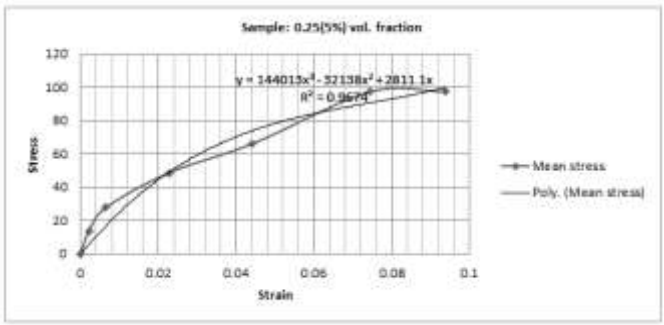

Fig-2: Stress – strain curve of compression test (1)

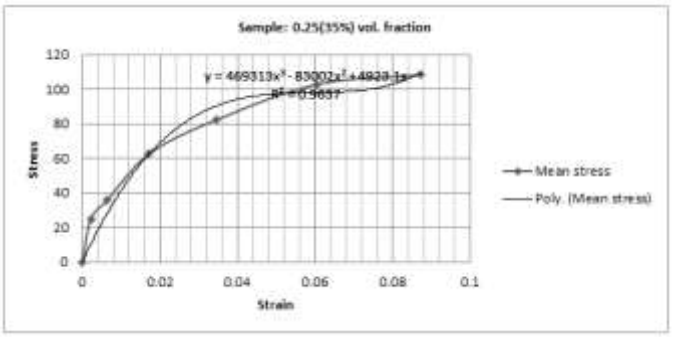

Fig-3: Stress – strain curve of compression test (2)

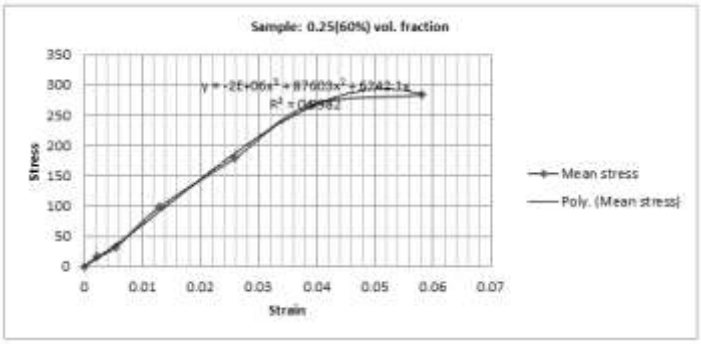

Fig-4: Stress – strain curve for compression test (3)

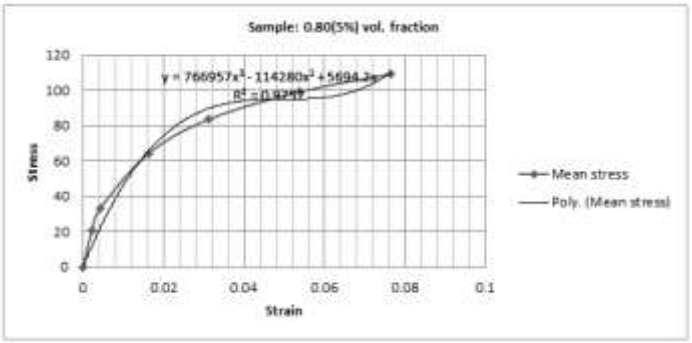

Fig-5: Stress – strain curve for compression test (4)

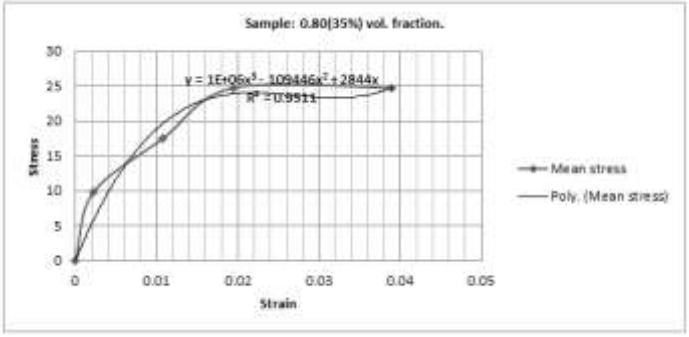

Fig-6: Stress – strain curve of compression test (5)

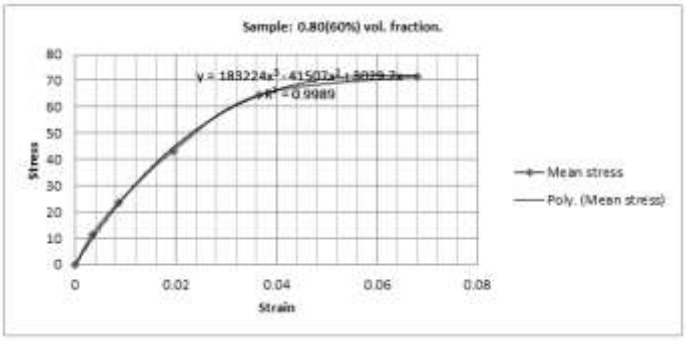

Fig-7: Stress –strain curve for compression test (6)

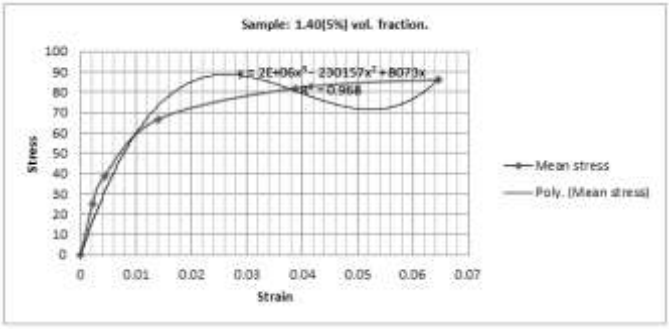

Fig-8: Stress – strain curve for compression test (7)

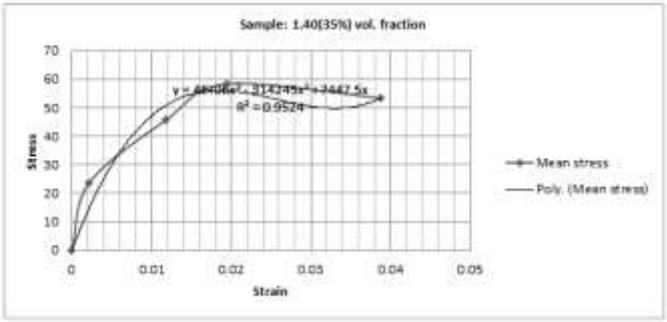

Fig-9: Stress –strain curve for compression test (8).

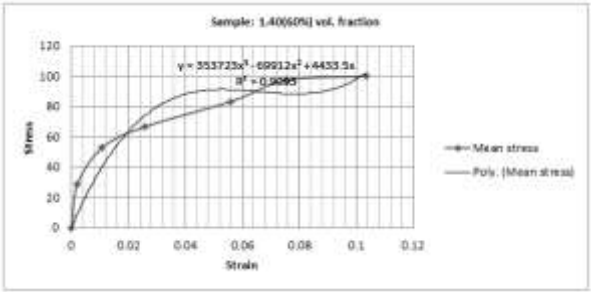

Fig-10: Stress – strain curve for compression test (9).

Calculating the area of Figure 3:

$$Y = 144013 \quad X^{3} - 32138 \quad X^{2} + 2811 \quad .1\,X \tag{1}$$

The area under the curve in the finite interval [a, b] is given as:

$$A = \int_a^b Y(X)\,dx \tag{2}$$

The area is determined using numerical approach for which Gauss – Legendre two-point rule states that:

$$\int_{-1}^{1} f(x)\,dx = f\left(-\frac{1}{\sqrt{3}}\right) + f\left(\frac{1}{\sqrt{3}}\right) \tag{3}$$

To apply this rule the finite interval [a, b] is changed to [-1, 1] using the transformation:

$$x = \left(\frac{b-a}{2}t\right) + \left(\frac{b+a}{2}\right) \tag{4}$$

By evaluating the area A_1, under the curve for which the finite interval [a, b] = [0, 0.094]:

$$A_1 = \int_0^{0.094} (144013\ \ x^3 - 32138\ \ x^2 + 2811\ \ .1x)\,dx \tag{5}$$

With the application of the transformation equation, we evaluate equation (4) with the finite interval to get:

$$x = \left(\frac{0.094\ - 0}{2}\right)t + \left(\frac{0.094\ + 0}{2}\right)$$

$$= 0.047\ (t+1) \tag{6}$$

$$dx = 0.047\ dt \tag{7}$$

Equation (5) is evaluated with the values of x and dx to give the transformed equation:

$$A_1 = \int_{-1}^{1} [144013\ \ (0.047\ )^3 (t+1)^3 - 32138\ \ (0.047\ )^2 (t+1)^2 + 2811\ \ .1(0.047\ )(t+1)]0.047\ \ dt$$

$$= \int_{-1}^{1} [144013\ \ (0.047\ )^4 (t+1)^3 - 32138\ \ (0.047\ )^3 (t+1)^2 + 2811\ \ .1(0.041\ )^2 (t+1)]\,dt$$

$$= \int_{-1}^{1} [0.702737499\ \ \ (t+1)^3 - 3.336663574\ \ \ (t+1)^2 + 6.2097199\ \ \ (t+1)]\,dt \tag{8}$$

By applying Gauss – Legendre two – point rule equation (8) becomes:

$$\int_{-1}^{1} f(t)\,dx = f\left(-\frac{1}{\sqrt{3}}\right) + f\left(\frac{1}{\sqrt{3}}\right)$$

$$f\left(-\frac{1}{\sqrt{3}}\right) = 2.0815533$$

$$f\left(\frac{1}{\sqrt{3}}\right) = 4.2510653$$

$$A_1 = f\left(-\frac{1}{\sqrt{3}}\right) + f\left(\frac{1}{\sqrt{3}}\right) = 2.08155337 \quad + 4.25106531 \quad = 6.33261868$$

$$\approx 6.3326$$

A_1 is the amount of energy absorbed or work done (J/m^2) on the unit volume of the material Before fracture.

Similarly Figure 3 – 10 were evaluated following the procedure adopted for Figure 2 with the finite intervals of the figures stated as follows:

Figure 3 has the finite intervals [a, b] = [0, 0.068] and [b, c] = [0.068, 0.088]

Figure 4 has the finite intervals; [a, b] = [0, 0.052] and [a, b] = [0.052, 0.058].

Figure 5 has the finite intervals; [a, b] = [0, 0.056] and [a, b] = [0.056, 0.077].
Figure 6 has the finite intervals; [a, b] = [0, 0.021], [a, b] = [0.021, 0.03] and
[a, b] = [0.03, 0.039]
Figure 7 has the finite interval; [a, b] = [0, 0.068].
Figure 8 has the finite intervals: [a, b] = [0, 0.026], [a, b] = [0.026, 0.053] and
[a, b] = 0.053, 0.065].
Figure 9 has the finite intervals; [a, b] = [0, 0.019], [a, b] = [0.019, 0.033] and
[a, b] = [0.033, 0.0385].
Figure 10 has the finite intervals; [a, b] = [0, 0.056], [a, b] = [0.056, 0.08] and
[a, b] = [0.08, 0.104].
With the evaluation of Figures 2 - 10, the energy absorbed by WARPP samples are presented in Table 4.

Table-4: Data of energy absorbed by the samples obtained from the evaluation of Figures 2- 10

Figure	$A_1 (J/m^3)$	$A_2 (J/m^3)$	$A_3 (J/m^3)$	$\sum A$
2	6.3326	–	–	6.3326
3	5.1914	2.0283	–	7.2197
4	8.8894	1.6490	–	10.5384
5	4.1244	2.1054	–	6.2298
6	0.3379	0.1594	0.0799	0.5771
7	3.6337	–	–	3.6337
8	1.6087	2.1524	1.0485	4.8096
9	0.7561	0.7206	0.2622	1.7390
10	3.7288	2.1488	2.2300	8.1077

Total work done on each sample of WARP

The area under the load displacement curve represents the total work done, and it can be Calculated by multiplying the area under the stress – strain curve by the volume of the sample. From the calculations presented in Table 4, the work done on the samples are presented in Table-5.

Table-5: Work absorbed by each sample at fracture

Figure	*Total energy* (J/m^3)	*Volume* (m^3)	$W(J)$
2	6.3326	0.000001044	0.0000066
3	7.2197	''	0.0000075
4	10.5384	''	0.0000110
5	6.2298	''	0.0000065
6	0.5771	''	0.0000006
7	3.6337	''	0.0000038
8	4.8096	''	0.0000050
9	1.7390	''	0.0000018
10	8.1077	''	0.0000085

Specific energy absorption (SEA)

Specific energy absorption is an important factor in the design of parts with high strength to weight ratio, such as vehicles, motorcycles, airplanes, etc. Specific energy absorption is the energy absorbed per unit mass of the sample or specimen. It can be calculated by dividing the energy absorbed by the sample with the mass of the sample. The result of the computation done for the WARPP samples is presented in Table 6.

Table-6: Specific energy absorption

Sample (with % vol. fractions of filler and matrix)	*W (J)*	*Mass (Kg)*	*SEA*
0.25 (5.92 *x* 94 .08)	0.0000066	0.00095	0.0069473684
0.25 (39 .44 *x* 60 .56)	0.0000075	0.00101	0.0074257426
0.25 (64 .52 *x* 35 .48)	0.0000110	0.00106	0.0103773580
0.80 (5.92 *x* 94 .08)	0.0000065	0.00095	0.0068421053
0.80 (39 .44 *x* 60 .56)	0.0000006	0.00101	0.0005940594
0.80 (64 .52 *x* 35 .48)	0.0000038	0.00106	0.0035849057
1.40 (5.92 *x* 94 .08)	0.0000050	0.00095	0.0052631579
1.40 (39 .44 *x* 60 .56)	0.0000018	0.00101	0.0017821782
1.40 (64 .52 *x* 35 .48)	0.0000085	0.00106	0.0080188679

Crush Force Efficiency (*CFE*).

This is a very important parameter in evaluation of the performance of structure during crushing process. CFE is the ratio between the mean crushing loads (force) F_{av}. and the maximum crushing load F_{max}., for each sample trial and can be obtained from the relation reported by Tao *et. al*. [11].

$$CFE = \frac{F_{av.}}{F_{max.}} \qquad (9)$$

Where F_{av}. = Mean crushing load

F_{max}. = Maximum crushing load.

And material with higher *CFE* will always be selected in design of energy absorbing system.
Equation (9) is evaluated for sample 1 of Table 3a having particle size, 0.25mm and volume fraction, 5%.

$$F_{av.} = \frac{1800 + 1700 + 1775 + 1750 + 1725}{5} = 1750$$

$$F_{max.} = 1800$$

$$\therefore CFE = \frac{1750}{1800} = 0.9722 \approx 97.22\ \%$$

Similarly *CFE* of other samples were calculated and their results are presented in Table 7.

Table-7: *CFE* for the nine samples of Table 3a with 5 replicates

Particle size (mm)	*Volume fraction (%)*	*Mean force ($F_{av.}$)*	*Maximum force ($F_{max.}$)*	*CFE (%)*
0.25	5	1750	1800	97.22
0.25	35	1950	2000	97.50
0.25	60	4800	5350	89.72
0.80	5	1965	2050	95.85
0.80	35	445	532	83.65
0.80	60	1290	1380	93.48
1.40	5	1550	1600	96.88
1.40	35	1050	1100	95.45
1.40	60	1800	1800	100

DISCUSSION OF RESULTS

The energy absorbed or work performed on the WARPP composites in compression were analyzed using Gauss – Legendre two point rules. The study showed that the energy absorbed at ultimate strength is in the range of 0.5771 J/m^3 – 10.5384 J/m^3 as was presented in Table 4, while Table 5 presented the value of total work done to be in the range of 0.0000006 J – 0.0000110 J. The values indicate that the materials did not absorb much energy before failure. Also Table 6 presented the highest value of specific energy absorbed as 0.01038 J/Kg. This energy absorption analysis is useful in selecting material to be used during the design of composite material for energy absorption.

The crush force efficiency was evaluated and presented in Table 7 above. The sample with a crush force efficiency of 100% demonstrates that the shape of force – crush distance curve is rectangular [12].

CONCLUSION

This study showed that the energy absorption of WARPP composites for two samples have the range of 3.6337 J -6.3326 J at ultimate strength/fracture, while seven samples had different ranges of energy absorption at ultimate strength and at fracture. The ranges are stated as 0.3379 J – 8.8894 J and 0.5771 J – 10.5384 J respectively. The specific energy absorption of 0.01038 J/Kg shows the sample with the highest strength – to – weight ratio. Also established by this study is the compressive modulus of 4.9885 N/mm^2.

Above all, material with the highest CFE will always be selected in design of energy absorbing systems, due to the energy management goal of absorbing all the energy without conveying or transmitting out large amount of force [12].

REFERENCES

1. Thornton P. H. (1979). Energy Absorption in Composite Structures. Journal of Composite Materials, Vol. 13 (7), 247- 262.
2. Ramakrishna S. and Hamada H. (1998). Energy Absorption Characteristics of Crashworthy Structural Composite Materials. Key Engineering Materials 141- 143, 585 – 619.
3. Hull D. (1991). A Unified Approach to Progressive Crushing of Fibre – Reinforced Composite
4. Ihueze C. C. & Enetanya A. N. (2012). Energy absorption and Strength Evaluation for Compressed Glass Fibre Reinforced Polyester (GRP) for Automobile Components Design in Crash Prevention Scheme. Journal of Minerals & Materials Characterization & Engineering, 11(1), 85 – 105.
5. Jacob G. C., Fellers J. F., Simunovic S. & Sarbuck J. M. (2002). Energy Absorption in Polymer Composite Materials for Automobile Crashworthiness. Journal of Composite Materials, 36 (7), 813 – 850.
6. Oberg E., Jones F. D., Horton H. L. & Ryffel H. H. (2012). Machinery's Handbook.29th Edition, Industrial Press, New York, p 566.
7. Robust Design: An Introduction to Taguchi Methods. https://www.ielm.ust.hk/dfaculty/ajay/courses/ielm317/lecs/robustdesign1.pdf (Accessed August, 2017).
8. Antony J. & Capon N. (1988). Teaching Experimental Design techniques to Industrial Engineers. *International Journal of Engineering Education, 14(5),* 335-343.
9. Aguh P. S. (2016). Evaluation of the Mechanical Properties of Wood Ash (Hardwood) Particles
10. Chapra S. C., and Canale R. P. (2006). Numerical Methods for Engineers. 5th Edition, McGraw- Hill, New York, pp 460 – 462 & 623 – 625.
11. Tao Y., Min Z. R., Jingshen W., Haibin C. & Ming Q. Z. (2008). Healing of Impact Damage in Woven Glass Fabric Reinforced Epoxy Composites. Journal of Applied Science and Manufacturing, 39(9), 1479 – 1487.
12. Rabiee A. and Ghasemnejad H. (2017). Progressive Crushing of Polymer Matrix Composite Tubular Structures: Review. Open Journal of Composite Materials, 7, 14 – 48.